DRAFT 12 January 1996 In Press Revised for Limnology and Oceanography

Appendix 5

The 1991 coccolithophore bloom in the central north Atlantic

II- Relating optics to coccolith concentration

William M. Balch

Bigelow Laboratory for Ocean Sciences, McKown Point, W. Boothbay Harbor, ME 04575

Katherine A. Kilpatrick

Division of Meterology and Physical Oceanography, Rosenstiel School for Marine and Atmospheric Science, University of Miami, 4600 Rickenbacker Causeway, Miami, FL 33149-1098

Patrick Holligan

Dept. of Oceanography, University of Southampton Highfield, Southampton, S017 1BJ, U.K.

Derek
~~Derrick~~ *Harbour*

Plymouth Marine Laboratory, West Hoe, Plymouth, PL1 3DH United Kingdom

Emilio Fernandez

Depto. Recursos Naturais e Medio Ambiente, Facultad de Ciencias del Mar, Campus Lagoas-Marcosende, Universidade de Vigo, E-36200, Vigo, Spain

Running head- Coccolithophore bio-optics

Abstract

This study summarizes the relationships between various biological and optical properties of a mesoscale coccolithophore bloom observed in the north Atlantic during June 1991. The optical properties were primarily affected by the concentration of coccoliths and suspended calcite. Backscattering was positively correlated to coccolith concentration and even better correlated with the concentration of suspended calcite. The reason for this was that it was difficult to enumerate the numbers of coccoliths attached to cells using microscopy whereas atomic absorption analyses of calcite-calcium were equally accurate whether calcite was attached or detached from cells. As the bloom aged, the ratio of detached coccoliths to plated cells increased. Dilution experiments provided the most precise relationships between coccolith backscattering and coccolith abundance. The calcite-specific scattering coefficient was estimated from measurements of beam attenuation, absorption, and calcite concentration. This average coefficient was close to theoretical estimates but there was some variability; at low cell and coccolith concentrations, the calcite-specific scattering coefficient was greatest. The ratio of scattering to absorption was partially driven by the ratio of calcite to chlorophyll in the seawater. The contribution of coccolith backscattering to total scattering was modeled as a function of coccolith concentration and chlorophyll concentration. Even at lower concentrations representative of "non-blooms", coccoliths are responsible for 5-30% of the total backscattering. Anomolous diffraction theory was used to show that calcite-specific scattering is the highest for 1-3μm spheres, the diameter of *E. huxleyi* coccoliths. The calcite-specific scattering coefficients of larger calcite particles (e.g. plated coccolithophore cells, foraminifera, pteropods) would be expected to be considerably lower. These data were used to test an approach for predicting coccolith concentration from water-leaving radiance in the blue and green wavelengths.

Acknowledgments

The officers and crew of the RRS Charles Darwin are acknowledged for their expert ship handling. The staff of the Research Vessel Services, Barry, U.K. are thanked for their logistical support of these ship studies. Beam attenuation data used to calculate total scatter were kindly provided by Charles Trees (CHORS, San Diego) and Roy Lowry (British Oceanographic Data Centre, Bidston, U.K.). Howard Gordon and Ken Voss (Univ. of Miami Physics Dept.) have provided help in data interpretation. The comments of two anonymous reviewers are greatly appreciated. This work was generously supported by ONR Ocean Optics Program (N00014-91-J-1048), NASA Global Biogeochemistry (NAGW 2426), NASA EOS/MODIS (NAS5-31363) and NSF Biological Oceanography Program (OCE-8900189 and OCE-9022227) to WMB. This paper is contribution #### to the U.S. Global Ocean Flux Program and contribution #### of the Bigelow Laboratory for Ocean Sciences.

Introduction

The advent of satellite remote sensing has highlighted some classes of algal blooms that significantly modulate the water-leaving radiance of surface waters. Blue-green algae such as *Trichodesmium* can cause high reflectance, beige-colored surface "slicks" in the tropics (Borstad et al. 1992; Lewis et al. 1988). Dinoflagellates can cause blooms or "red tides" in shelf waters at frontal-scales (Pingree et al. 1975; Holligan 1984). Intense green open-ocean diatom blooms also have been observed from space at frontal scales in central ocean basins (Yoder et al. 1994). Coccolithophore blooms, first recognized in satellite images about a decade ago (Holligan et al. 1983), turn the ocean a milky turquoise color and have been observed in both coastal waters and the open ocean. Coccolithophores are members of the algal class Prymnesiophyceae which produce calcium carbonate scales called coccoliths. These range from 1-10μm in diameter and have various shapes such as rhombahedral crystals, discs (with and without a central hole and/or radial elements), and "trumpet" shapes (Reid, 1980). Coccoliths are first attached to the cells and later detach into the seawater.

The main optical impact of coccoliths is to increase the light scattering. Here, we are referring to particle scattering (as opposed to Rayleigh scattering) where the wavelength of light is less than, or equal to, the particle size. Such light scattering is mainly in the forward direction and is size dependent. That fraction of light scattered in the backwards direction per unit thickness is termed backscattering (b_b). (See Table 1 for complete list of symbols used in this work and their definitions). Volume scattering functions of homogeneous particles in the visible wavelengths (λ) are a function of 1) the spectral value of the real part of the particle's refractive index (n), the spectral value of the imaginary part of the refractive index (n', where $n' = a\lambda/4\pi$, and a is the absorption coefficient), and the particle size distribution. There are relatively few values of n and n' available in the literature for coccolithophores (but see Morel 1987 and Bricaud et al. 1992). The high index of refraction of calcite relative to water makes it an extremely efficient scatterer of

light. Given that coccoliths do not absorb light at visible wavelengths (Balch et al. 1991), then the imaginary part of their refractive index is zero.

Four features that set coccolithophore blooms apart from other monospecific blooms of non-calcifying algae are 1) the optical signature is mostly controlled by light scattering from detached inorganic coccoliths, not absorption and scattering by particulate organic matter, 2) organic biomass is often relatively low, 3) coccolithophore blooms are observed at one part of the organism's life cycle, when its plates are detaching, and 4) these blooms impact significantly larger areas than most other types of monospecific blooms. Areal extents of typical coastal coccolithophore blooms are 50,000 to 100,000 km^2 (Holligan et al. 1983; Balch et al. 1991; Brown and Yoder 1993) while open ocean blooms have been observed to have areas > 0.5 x 10^6 km^2 (Holligan et al. 1993).

Coccolithophores affect not only the optics, but also the seawater chemistry; in high abundance, they strongly modulate the alkalinity and ΣCO2 levels in surface waters (Robinson et al. 1994). Such chemical changes frequently parallel optical changes. For example, alkalinity in coccolithophore blooms has been shown to be inversely related to optical backscattering of detached coccoliths. Moreover, beam attenuation has been shown to be positively related to PCO_2 (Holligan et al. 1993).

Coccolithophore blooms also impact other aspects of biology in the euphotic zone. For example, due to their ability to survive in moderately stratified, low nutrient waters, coccolithophores can out-compete diatoms for nutrients in such conditions. Thus, they represent "transitional" species between well-mixed, diatom-dominated waters and well-stratified, dinoflagellate-dominated waters (Margalef 1979). Moreover, due to their ability to increase the light scatter of surface waters by detaching their coccoliths, they shoal the euphotic zone, which lowers the light availability for deeper algal species. In turn, this may allow the nitracline to shoal because nitrate uptake is often light-dependent (MacIsaac and Dugdale 1972).

Even though the optical scattering by coccoliths can be significant, there are still relatively few studies that define the precise relationship between the coccolith abundance and light scattering. Earlier studies showed that the relationship between coccolith concentration and light scatter was highly significant, but with variance associated with growth phase of the cells and/or coccolith detachment rates (Ackleson et al. 1994; Balch et al. 1991). The exact nature of the growth effects has remained unknown for field populations.

The first paper of this series examined the spatial variability of optical properties in a mesoscale coccolithophore bloom in the north Atlantic Ocean (Balch et al. submitted). This second paper of the series relates the optical properties (backscattering and total light scattering) to the coccolith abundance, suspended calcite concentration and particle size in this 0.5 x 10^6 km^2 bloom. We applied simple models to explain the effects of chlorophyll and calcite on inherent optical properties of absorption and scattering in seawater. Dilution experiments were used to definitively relate backscattering to coccolith concentration at a given location within the bloom. The light scattering results are compared to predictions based on calcite spheres of various sizes.

Methods

Observations were made on cruise 60 of the RRS *Charles Darwin* (CD60) from 13 June to 3 July, 1991. The cruise track can be found in Balch et al. (submitted; figure 1). Two transects were made along the 20°W and 15°W meridian. Detailed optical measurements of volume scattering and absorption were performed at 111 and 210 stations respectively. For comparative purposes, the ship visited a site well outside the bloom (59° 39' N x 20° 59' W; site of an optical mooring). Other cruise details can be found in Holligan et al. (1993). The reader is referred to Balch et al. (submitted) for details of the methodology for measuring total light scattering (b), backscattering (b_b), and particulate absorption (a_p), all at 436nm and 546nm wavelengths. Briefly, backscattering due to

calcite, hereafter called bb', was calculated as the difference between the b_b of raw seawater and the b_b of the same sample following 30s of bubbling with CO_2 (which reduced the pH to 5.5 and dissolved the calcium carbonate).

Dilution Experiments

Water was sampled using a Niskin bottle, and transferred to a 1 liter polyethylene bottle. A 100 milliliter aliquot of seawater was serially diluted with 0.2μm filtered seawater to achieve a series of coccolith concentrations. Then, volume scattering was measured and backscattering calculated for each concentration.

Total Particulate Carbon and Calcite Analyses

Total particulate carbon was measured according to Fernandez et al. (1993). The technique involved filtering 0.5 liter seawater through precombusted Whatman GFF filters and freezing at -20°C. A Carlo-Erba 1500 (series 2) CHN analyzer was used to measure the total carbon, with no pretreatment to remove calcium carbonate. Calcite was measured by first filtering seawater on pre-combusted Whatman GFF filters, then measuring the atomic absorption of calcium using the technique described by Holligan et al (1993). This technique assumes that all particulate calcium is in the form of calcium carbonate. Briefly, one liter samples were filtered through pre-combusted Whatman GFF 25mm filters, the filters were rinsed with several washes of filtered seawater before freezing at -20°C. Samples were extracted by adding 2 milliliter of 50% trace-metal-clean hydrochloric acid to tubes containing the filters. They were incubated overnight at 40 ^{0} C in a water bath. 8 milliliters of 1% lanthanum chloride was added to each tube (to remove phosphorous suppression of ionization). The supernatant was then injected into a flame photometric atomic absorption spectrometer, measuring absorption at 422.7 nm with a 10 cm air-acetylene flame. Calibration curves were prepared using commercial calcium standards. Blank filters were prepared towards the end of the cruise by mounting identical pre-

combusted filters in the filter tower apparatus, applying vacuum, and adding GFF filtered seawater to wet the filter, and identical rinsing and preparation techniques as described above. Total organic carbon was estimated as the difference between total particulate carbon and inorganic calcite carbon.

Cell and Coccolith Enumeration

Cell and coccolith enumeration was performed according to Holligan et al. (1984). Counts were performed on both buffered formalin and Lugol's iodine using an inverted microscope.

Results

Standing stocks of cells, coccoliths and carbon

There were some well-defined patterns that were observed in the cell count and particulate analyses during the meso-scale coccolithophore bloom. Coccolith concentrations [N_{cocco}] were about an order of magnitude higher than coccolithophore cell concentrations [N_{cells}]. Note, however, that the ratio of coccoliths to cells was not constant; a least-squares linear fit only explained 53% of the variance with the standard error of the dependent variable [N_{cocco}] of 45259 coccoliths/milliliter. A least-squares power fit explained considerably more variance (78%) and the relationship, plus error terms, is given in Table 2. It implies that the ratio of detached coccoliths to cells was decreasing from 26 to 17 as cell abundance increased from about 100 to 10,000 cells milliliter^{-1} (Fig. 1A). The standard error of the dependent variable (Log [N_{cocco}]) was +/- 0.31 log units or about a factor of 2.

A comparison of total particulate carbon versus calcite carbon concentrations revealed that the techniques were internally consistent; in all cases (save for one), total particulate carbon always exceeded calcite carbon. While there was not a highly significant relation between total and calcite carbon, the typical ratio of total particulate carbon:calcite

carbon varied between 2-6 with values approaching 1 as the calcite concentration increased (data not shown). Plotting calcite carbon concentration ([C_{CaCO3}] in $\mu g\ liter^{-1}$) versus the coccolith concentration (per $milliliter^{-1}$) provided an estimate of the carbon per coccolith. The least-squares relationship is given in Table 2 (Fig. 1B).

Backscattering and scattering as a function of suspended calcite

The blue and green b_b' values represent only the backscattering due to calcium carbonate, with no particulate organic carbon. Our results of comparisons between b_b' versus the numbers of coccoliths or concentration of calcium carbonate are presented in Table 2. The size of the data set for comparison of b_b' and calcite concentration was bigger than the data set for comparison of b_b' and coccolith concentration (due to the time-consuming nature of microscopic cell counts). It is not apparent that this produced any bias to the results, however, since calcite concentration and coccolith abundance were sampled throughout the bloom. Highest coefficients of determination and lowest standard errors resulted when b_b' was predicted from calcite concentration (Table 2, Fig. 2). Reasons for this will be discussed later.

The best relationships between b_b' and coccolith concentration were achieved during the dilution experiments. In seven experiments using water from the top 12m, the average coefficient of determination was 0.96 for all 436 and 546nm measurements (Table 3, Fig. 3). Moreover, the slopes of the b_b' versus coccolith relationships varied by about 4X at either wavelength, with the largest slopes observed early in the event (22, 24, and 25 June), and reduced values at the end of the bloom (6/27 and 6/29).

Beam attenuation (c) was measured along-track and in vertical profiles during the bloom (see description in Balch et al. submitted). Given that beam attenuation is the sum of scattering (b) and absorption (a), it was possible to calculate total scatter as the difference between c and a, where total absorption was taken as that due to water and particles only (Balch et al. submitted). Note, that the scatter due just to calcite (b'; m^{-1}) could not be

calculated using this technique, since the treatment to dissolve coccoliths could not be performed in situ, in the volume viewed by the transmissometer. Nevertheless, there was a positive relationship between total scatter (b_{436} or b_{546}) versus calcite concentration which was well fit by the linear relationships given in Table 2 (see also Fig. 4). For relating calcite concentration to light scatter, the green wavelengths are preferred to the blue wavelengths as the impact of chlorophyll absorption is minimized. For the b_{546} vs. $[C_{CaCO3}]$ relationship in Table 2, the Y intercept (0.410 m^{-1}) was significantly different from zero and had confidence limits of 0.29 to 0.53 m^{-1}. The slope of this line, 8.413×10^{-3} m^2 (mg calcite C)$^{-1}$ represented the calcite-specific scattering coefficient (b^*_{550}). The 95% error limits on the slope were 7.49×10^{-3} to 9.33×10^{-3} m^2 (mg calcite C)$^{-1}$ and there was some bias in the error, with highest b^*_{550} values at low coccolith concentrations (Fig. 5).

Scattering per unit chlorophyll was calculated for comparison to the large numbers of historical data collected by Morel (1987); such values were generally 10X greater in this coccolithophore feature than in typical non-bloom populations, and there was no correlation between chlorophyll and light scattering. A different approach for accounting for the absorption and scattering values in this coccolithophore bloom was to compare the ratio of scattering to absorption (b/a) to the ratio of the concentrations of the principal scatterer to the principle absorber (mg calcite C/ mg chlorophyll, hereafter designated γ). It should be noted, however, that the correlation was lower than expected; it was strongest at 550 nm, but still accounted for only 43% of the variance. Using only data where b/a>10 (as representative of the most turbid parts of the bloom), the b/a ratio versus γ least squares fit accounted for 62% of the variance (Table 2). At 436nm, the correlations between b/a versus γ never exceeded r^2 of 0.44 (data not shown).

Discussion

From a remote sensing perspective, the time scale for the onset of turbid conditions was driven by three factors, the calcification rate, the coccolith detachment rate, and

numbers of coccoliths per coccolithophore. Numbers of coccoliths per cell have been previously estimated at about 15 for *E. huxleyi* (Paasche, 1962). Linschooten et al. (1991) also found that *E. huxleyi* in a 16:8 light dark cycle, grown on full-strength IMR medium (Eppley et al., 1967) had 15-20 coccoliths per cell at the end of the light period. They pointed out that this number of coccoliths was sufficient to cover the cells in a single layer. Our previous estimates (Balch et al. 1993) have shown that numbers of coccoliths can reach as high as 80 per cell at mid-logarithmic growth, and this decreases as cells reach stationary phase. Using just coccolith and cell size, we previously calculated that the first layer of plates consists of about 15 coccoliths. The relationship between detached coccolith abundance and cell abundance from this North Atlantic bloom was similar to previous laboratory studies (Balch et al. 1993); on average, each cell detached a maximum of 26 coccoliths, or almost two layers, during the early stages of growth and a minimum of 17 , or about one layer, towards the later stages of the bloom (Fig. 1; Table 2). Note, this should not be confused with the results of Fernandez et al. (1993; their table 1) who showed that the coccolith/cell ratio in the same bloom varied about one order of magnitude at 5 stations, from 12 to 108. The ratios cited here are the average values derived from *all* the cell counts shown in figure 1. For example, using the 95% confidence intervals for slope and intercept of the first regression in Table 2 (Log coccoliths versus Log coccolithophores) would give a range in coccoliths/cell of 11 to 65 when there were 100 cells milliliter^{-1}, and a coccolith/cell ratio of 5 to 61 when the cell concentration was 10,000 cells milliliter^{-1}. These ratios for the entire data set are a bit lower than at the five stations cited by Fernandez et al. (1993).

The fact that the ratio of detached coccoliths per cell varied, plus the observation of other phytoplankton species, undoubtedly caused large variance in ratios of total particulate carbon to calcite carbon. In the less concentrated parts of the bloom, calcite carbon represented about 16-50% of the total carbon, whereas in the densest part of the bloom, virtually all of the carbon was as calcite which leads to the question, where did the organic

carbon of the coccolithophores go? Cell lysis may have occurred but there was little evidence for unusual numbers of viruses in the late bloom stages (see Bratbak et al. 1993). It seems equally probable that the lack of organic carbon was due to highly efficient removal by grazers or sinking (Holligan et al., 1993).

The calcite concentration data, combined with coccolith count values (Fig. 1B), provided an opportunity to check the calcite carbon per coccolith for field populations of *E. huxleyi*. Previous laboratory and field studies have shown this to be variable. For example, Paasche (1962; 1963) gave a value of 0.17 pg C per coccolith for cultured cells. Linschooten et al. (1991) estimated less than half this value, 0.065-0.078 pg C per coccolith. Balch et al. (1991) estimated 0.26 pg C per coccolith based on CHN measurements of field populations. Holligan et al. (1983) saw distinctly higher values of 0.5 and 0.6 pg C per coccolith. The least squares fit to the data of Figure 1B gave 1.05 pg C per coccolith but this high value resulted from the fact that coccoliths attached to cells were not included in the coccolith count. When the coccospheres were multiplied by 20 (assuming 20 coccoliths per cell) and added to the detached coccolith concentration, the calcite per coccolith reduced to 0.47 pg C per coccolith (Fernandez et al. 1993), more reasonable, but still higher than results from previous laboratory studies. This calculation also implied that, on average, over half of the coccoliths were detached in the North Atlantic bloom of 1991. This has important ramifications for interpreting the light scatter data.

Relation of backscattering to coccolith concentration

Two fundamentally different approaches were used to understand the impact of coccolith density on calcite-dependent backscattering (b_b'). The first involved measuring b_b' of seawater samples and plotting it against coccolith concentration with no dilution (Fig. 4). Hereafter, this will be referred to as the "nondilution approach". Note, in making

these regressions, data is pooled from various locations within the bloom, regardless of growth stage.

Our past experience has shown that calcite backscattering varies not simply as a function of coccolith density. Other factors may be involved, such as the number of detached versus attached coccoliths, variance in the abundance of other calcifying algal species, coccolith size, and coccolith integrity. All of these factors may vary as a function of the growth stage of the bloom.

The second approach used in this work involved serial dilutions of individual samples and examining b_b' against coccolith abundance (hereafter called the "dilution approach"). The purpose of the dilution experiments was to examine the relationship between calcite-specific backscattering versus coccolith concentration for specific stages of bloom development. The results from the dilution experiments allowed deductions about how much variance in the b_b' versus coccolith relationship could be attributed to growth stage. The results allowed limited speculation on the cause of the variations; for example, they did *not* discern between coccolith integrity and coccolith size. Since this analysis only focused on b_b', not b_b, potentially complicating factors related to other organic particles was not invoked to interpret the results. For example, changes in refractive index would not have been expected to cause changes in b_b' (unless calcite particles had been replaced with aragonite particles, for which there was no evidence from our microscopy).

Based on the nondilution approach, 80-85% of the variance in b_b' could be accounted for by the abundance of detached coccoliths in the Gulf of Maine (Balch et al. 1991). In the North Atlantic coccolithophore bloom, only 56-63% of the variance in b_b' could be explained using the non-dilution approach (Table 2). For the BOFS expedition, use of the dilution approach increased the explained variance another 30-40% (to >95%) for 11 out of 14 individual experiments (Table 3; Fig. 3). Two exceptions with lower explained variance were at the station at 60.9°N x 23.9°W on 25 June. The results of this dilution experiment were notably curvilinear. Multiple scattering is difficult to invoke as a

reason for the curvilinear behavior since the detached coccolith concentration was not particularly high to begin with, certainly no higher than other experiments where the relationship was clearly linear. The other low r^2 value was associated with the 546nm data at the station on 27 June (61.2°N x 15.2°W; r^2=0.84). This appears to be due to one anomalous data point at 2.25 x 10^7 coccoliths $liter^{-1}$. Note, the 436nm data at the same station were highly linear (r^2=0.99) which supports the possibility that the 546 nm data had a bad data point. Overall, the dilution experiment results clearly showed the differences in the b_b' vs coccolith relationship for different parts of the bloom. We speculate that the most likely cause of the high variance between dilution experiment "slopes" were differences in the ratio of detached coccoliths to plated cells which varied with bloom age. Nevertheless, we cannot exclude changes in coccolith integrity or the size distribution of the coccoliths (the latter admittedly being one of the most important factors affecting light scattering of marine particulates).

We estimated the age of this bloom from the earliest satellite image where no high reflectance water was observed (June 10, 1991), and by the next available image (15 June, 1991) the bloom was well underway. The assumption of a 10 June start date may cause a slight overestimate in the age. For the dilution experiment data, we observed that the detached coccolith/cell ratio increased with bloom age (Table 4). Moreover, as the detached coccolith/cell ratio increased, the slopes from the dilution experiments--essentially the backscattering per detached coccolith-- decreased (Fig3).

Many of the above problems can be avoided by using the mass of calcium carbonate instead of numbers of coccoliths, to quantify coccolith abundance. Use of the non-dilution approach, but regressing bb' against calcite concentration, explained about 85% of the variance in b_b' *for all cruise samples* (Fig. 2). This tighter fit probably was due to the fact that coccoliths attached to cells were included in atomic absorption estimates but they were not included in microscope enumeration.

Calcite concentration explained 70% of the variance in total scatter (b_{546}; Fig. 4). This was due to two reasons: 1) estimates of b_{546} were based on the difference between beam attenuation and absorption, and measurement errors likely were greater for b than they were for b_b' and 2) the data included scattering from other types of non-calcite particles. Another factor which may have affected the relationship between calcite concentration and light scattering, was particle size. This will be addressed later.

Calcite, chlorophyll and b/a

Kirk (1981a &b) used a Monte Carlo approach to demonstrate that the ratio of b/a is proportional to Kd(zm)/a (vertical attenuation coefficient for downward irradiance at the mid-point of the euphotic zone divided by the absorption coefficient). Hereafter, the euphotic zone is defined as the depths where downward irradiance >1%. The relationship also included two other factors, μ_0, the cosine of the zenith angle of refracted solar photons just beneath the surface, and $G(\mu_0)$, the fraction of scattering to vertical attenuation (determined from the scattering phase function). Kirk's semi-empirical relationship is given below.

$$Kd(zm)/a = 1/\mu_0 [1 + G(\mu_0)\, b/a]^{1/2} \qquad (1)$$

Kirk (1991) applied a similar Monte Carlo analysis to 7 different water types of widely variable volume scattering functions (Petzold 1972). He showed that the equation 1 was generally applicable. Moreover, assuming that the incident light was vertical (μ_0=1), replacing Kd(zm) by Kd(avg) (the average Kd above the depth where downward irradiance = 1% of the surface value), he showed that G(1) was approximately constant with a coefficient of variation of 3.9%. The specific value of G(1) from San Diego Harbor based on Petzold (1972) was 0.231; this is highly relevant to this work since San Diego Harbor has been shown to have a volume scattering function very similar to a previously

observed coccolithophore bloom (Balch et al. 1991). Equation 1 therefore can be re-written.

$$Kd(avg)/a = [1 + 0.231\ b/a]^{1/2} \quad (2)$$

Equations 1 and 2 yield plots of Kd/a versus b/a that are slightly curvilinear (concave-down) up to b/a of 30. For the limit value of b/a =0 (only absorption, no scatter), Kd(zm)/a equals 1.0 (Kirk 1991; his Fig. 1). To illustrate the role of coccoliths in increasing the effective pathlength of light moving vertically through the water column, we have substituted our b/a values into equation 2. In the north Atlantic coccolithophore bloom, 87% of the b/a values at 550nm exceeded 5, and 62% exceeded 10 with the peak b/a values of 45. Therefore, we would expect that Kd(avg)/a values fell between approximately 1.5 and 3.4.

The b/a ratio in typical phytoplankton blooms is usually a function of chlorophyll, but as already discussed, b/a at 546 nm in this coccolithophore bloom was mostly a function of γ, especially in the densest parts of the bloom. The slope of the relation between γ and b/a at 550 nm in the most turbid regions (b/a>10) was about 0.06 mg Chl/mg calcite (Table 2).

To check for internal consistency between the observed inherent optical properties and the quantity of calcite and chlorophyll, the following can be written, specifically for turbid parts of this bloom where b/a>10.

$$b/a = (b^* \times CaCO_3)/(a^* \times Chl) > 10 \quad (3)$$

Equation 3 was then rearranged, substituting γ, to give equation 4, again applicable only to the turbid parts of the bloom.

$$(10a^*)/b^* < \gamma \quad (4)$$

Based on previous calculations of a* and b*, the left side of equation 4 equaled 15.33 mg calcite C/mg Chl [= (10 x 0.0129 m^2(mg Chl *a*.)$^{-1}$)/8.413x10^{-3} m^2 (mg calcite C)$^{-1}$]. As expected, γ values in the coccolithophore bloom fell above this value 97% of the time. Moreover, the slope in the plot of γ versus b546/a546 for all data where b/a>10, was 0.059 mg Chl/mg calcite C (Table 2), representing a statistical average of all of our data. The reciprocal of this slope (16.9 mg calcite C/mg Chl) fell within 10% of (10a*)/b*.

Modelling light scatter due to coccoliths

Our field results provided the means to assess the magnitude of calcite-dependent light scattering relative to the total backscatterance of seawater. The calculations were done two ways, based either on coccolith-specific backscattering or calcite-specific backscattering. There were several assumptions required, however: 1) we used 1.84x10^{-13} (m^2 coccolith)$^{-1}$ and 1.35x10^{-13} (m^2 coccolith)$^{-1}$ for the coccolith-specific backscattering coefficients at 436 nm and 546 nm, respectively (slopes in row 3 and 4, of Table 2), 2) we used the slopes from rows 5 and 6 of table 2 to calculate the calcite-specific backscattering coefficients, and 3) backscattering due to water was 2.27x10^{-3} and 0.965x10^{-3} m^{-1} for 436 nm and 546 nm, respectively (Gordon et al. 1980).

The backscattering due to chlorophyll involved two calculations. The first calculation was based on an earlier bio-optical model of Gordon (1987), designed for case I waters (that is, waters where optical characteristics are dominated by algae and their associated detritus). Particulate scattering at 550 nm (b_p(546)) was empirically predicted using a relationship from Gordon and Morel (1983; based on 550 nm light):

$b_p(550) = Bc\ C^{0.62}$

where B_C represents the scattering coefficient when the concentration of chlorophyll plus phaeopigment (C) is 1 mg m^{-3}. Typically, B_C ranges from 0.12-0.45, with an average of 0.3. Moreover, Gordon (1992) incorporated three factors into their model: 1) that detritus scatters inversely with wavelength, 2) phytoplankton scattering is much less wavelength-dependent, and 3) the wavelength-dependent effects are most pronounced at low C while at

high C, b is essentially wavelength-independent. The relationship derived to satisfy the above observations was (Gordon 1992; his eqn 14):

$$b_p(\lambda) = (0.3\ Chl^{0.62})\ [[(0.5 + (0.25 \log Chl)) + (0.5 - (0.25(\log Chl)))]\ 550/\lambda) \quad (5)$$

where λ represents the wavelength in nanometers. Next, the ratio b_b/b, or $\tilde{b}_b$, has been empirically related to chlorophyll at the two wavelengths by Gordon and Morel (1983; their p. 62).

$$\tilde{b}_b\ chl\ 436 = 1.005\ (Chl^{-0.404})\ 0.01 \quad (6)$$

$$\tilde{b}_b\ chl\ 560 = 1.009\ (Chl^{-0.262})\ 0.01 \quad (7)$$

Note that equation 7 applies to 560 nm, not 546nm but the effect of this difference will be minor. Also, both equations 6 and 7 include multiplication by 0.01 because the original equations provided $\tilde{b}_b$ values in percent (Gordon and Morel 1983). The value $b_{bchl}(\lambda)$ was taken as the product of $b_{chl}(\lambda)$ and $\tilde{b}_b\ chl\ (\lambda)$.

$$b_{bchl}(\lambda) = (b_{chl}(\lambda))\ (\tilde{b}_b\ chl(\lambda)) \quad (8)$$

The results of this modeling can be seen in figure 7 along with data from the bloom. As chlorophyll increased, chlorophyll backscattering increased according to equations 6-8. Thus, the fraction of total backscattering attributed to coccoliths would have decreased purely due to the percentage of organisms containing chlorophyll relative to those containing calcite. It is readily acknowledged that backscattering can be strongly influenced by absorption in phytoplankton (Morel and Bricaud 1980) and the two variables are not necessarily independent. To this end, the above equations relating chlorophyll to

backscattering are empirical, and therefore implicitly include effects of chlorophyll absorption. The relationship between b_b'/b_b vs. coccolith concentration or calcite concentration was curvilinear on a log-log plot with the lines converging towards higher coccolith concentrations. It can be seen that at low chlorophyll concentrations (say 0.1μg chl *a* liter^{-1}), a coccolith concentration of 2000 coccoliths ml^{-1} is sufficient to increase the calcite-dependent scatter to 10% of the total scatter at 546 nm. At a concentration of 10,000 coccoliths ml^{-1} (still considered "non-bloom"), coccoliths represent about 35% of the total b_b at both wavelengths. Values of b_b'/b_btot are 50% between coccolith concentrations of 20,000-40,000 coccoliths ml^{-1}, depending on the chlorophyll level.

The data and predictions for b_b'/b_btot showed values of 50% between calcite concentrations of 40-80 μg calcite C l^{-1}, depending on the chlorophyll level. The model predictions agreed with data mostly at high coccolith densities and there was considerable error at lowest coccolith densities. Cruise data (plotted on the same figure) often fell outside the expected range for water containing 0.01 to 10 mg chl *a* l^{-1}, especially at 436nm wavelength. Clearly, given the variance in coccolith-specific backscatterance (Fig. 3) and calcite-specific backscatterance (Fig. 2), this might account for some of the problem. Furthermore, equations 6, 7 and 8 are average relationships for predicting backscattering from chlorophyll, which also have large confidence limits. Failure of the data to fall within the bounds set by the different chlorophyll levels in figure 7, may be as much due to reduced accuracy of the chlorophyll-component of the model. Regional relationships for these equations might be one solution to this problem. This model only begins to describe the envelopes of variability of calcite-dependent scatter as a function of the concentrations of coccoliths, calcite or chlorophyll *a*. Clearly, more refinements are necessary.

As a cross-check of the scattering coefficients observed in this field study, we calculated calcite-specific scatter for calcite spheres based on anomalous diffraction theory for non-absorbing spheres of van de Hulst (1981; his p. 176). Morel (1987) defined the

attenuation efficiency factor (Qc) as a function of the dimensionless parameter ρ, which is a function of particle diameter (d), wavelength (λ), refractive indices of water (n_w=1.33; Jerlov 1976) and of calcite (n=1.583; Aas 1981). The refractive indices then were used to calculate the relative refractive index (m=n/nw=1.19 for coccoliths).

$$\rho = 2\pi\,(d/\lambda)\,(m-1) \qquad (9)$$

Next, ρ was used to approximate the efficiency of attenuation.

$$Qc(\rho) = 2 - (4/\rho)\sin\rho + (4/\rho^2)(1-\cos\rho) \qquad (10)$$

This function was derived for particles where $2\pi\,(d/\lambda) >> 1$ and the quantity $(m-1) << 1$. For coccoliths, the value of $2\pi\,(d/\lambda)$ at 550nm is 11-23. As described by van de Hulst (1981), equation 10 models light extinction not only when m is close to 1 but even up to values of m= 2 (see figure 32 of van de Hulst 1981; p. 177). Calcite is effectively non-absorbing, so its absorption efficiency, Qa, is zero and its scattering efficiency, Qb, dominates the attenuation efficiency. (That is, Qc = Qa + Qb, so with calcite particles, Qc = Qb). The calcite specific scattering coefficient was calculated by applying equations 9 and 10 to the following equation (Morel 1987):

$$b^* = (3\,\pi/c_{calcite}\,\lambda)\,nw\,(m-1)\,Qb(\rho)/\rho \qquad (11)$$

where $c_{calcite}$ was the density of calcite (2.711×10^6 g m^{-3}). These calculations were performed for calcite spheres from 0.1-1000 mm. Note, equation 10 can be used to calculate the efficiency of attenuation (or in this case the efficiency of scatter) provided that $\pi d/\lambda$ exceeds 1. For these calculations, this would occur at a diameter of 0.14 μm, thus the abscissa of Fig. 7 begins at 0.1 μm. The calcite specific scattering coefficient (b*; m^2(mg calcite C)$^{-1}$) peaked at diameters between 1-3 μm, precisely the size range of

Emiliania huxleyi coccoliths (Fig. 7). From this approach, a 2 μm calcite sphere should have a b* of 9.7x 10^{-3} m^2(mg calcite C)$^{-1}$.

The average observed calcite-specific scattering coefficient for 2 μm coccoliths (b*=8.4 x 10^{-3} m^2(mg calcite C)$^{-1}$; Fig. 4) was 13% lower than the theoretical value of b* for a 2 μm calcite sphere ($P<0.01$). This may have been related to the effect of shape on calcite scatter (discs versus spheres). Size differences also may have caused the error limits in the slopes of Fig. 4 (2 S.E. about these slopes represented +/-8%; Table 2, rows 5 and 6). As already shown, theoretical results for calcite spheres suggested that calcite-specific scatter should increase with decreasing size, peaking at a diameter of 1 μm, and declining below this size (Fig. 7).

It is also worthy of note that we observed slightly higher b* values at low calcite concentrations. This may have resulted from differences in calcite particle size or shape when the concentration of suspended calcite was low versus high (see also Aas 1984). It is important to caution, however, that there was a cluster of b^*_{550} values at early bloom stages (2 x 10^{-2} m^2 (mg calcite C)$^{-1}$) which were *above* the theoretical value for calcite spheres. This may have been due to other calcite-containing species contributing a significant fraction of the total scattering, such as *Coccolithus pelagicus*, but this remains speculative.

The peak of the theoretical b* vs size relationship of Fig. 7 was about 1.25 μm (b*= 1.19x10^{-2} m^2(mg calcite C)$^{-1}$). This has interesting ramifications towards understanding which calcite particles cause the most scatter in the sea. Most coccoliths, including those of *E. huxleyi*, are 1-2 μm in diameter which, provided their scattering behavior is similar to that of calcite spheres, would give them high calcite-specific scattering efficiency. Moreover, one would expect lower calcite specific scattering coefficients for calcite particles <1 μm and > 3 μm, which implies that, per unit mass, coccoliths are likely more important modulators of ocean scatter than plated coccolithophore cells, or the larger calcite tests of foraminifera or pteropods (>100 μm diameter). Fig. 7

shows the size ranges of these other calcium carbonate particles found in the sea for comparison, .

Heretofore, it has been difficult to ascribe any significance to the morphology of coccoliths. We only can speculate from these results that producing turbid conditions may be somehow selectively advantageous to coccolithophores. If so, natural selection may have resulted in calcite scales with peak light scatter per unit mass. We previously hypothesized (Balch et al. 1991) that shedding highly scattering plates into the water increases the effective pathlength of light within surface waters, increasing the probability of photon capture by the coccolithophores and decreasing the probability of photon capture for deeper species of the chlorophyll maximum. The results here further support this hypothesis.

The results presented in this work also aid attempts to estimate the concentration of calcite coccoliths from space. Water-leaving radiance (Lw) and reflectance are strongly related (Gordon and Morel 1983) and reflectance is a function of $b_b/(a+b_b)$ (Gordon et al. 1988). Thus, bb/(a+bb) is a good proxy for Lw. We therefore plotted $b_b/(a+b_b)546nm$ versus $b_b/(a+b_b)436nm$ and contoured isopleths of coccolith density and chlorophyll *a* (Fig. 8). The results showed that the isopleths of coccolith concentration were almost horizontal while the chlorophyll isopleths ran more diagonally. In other words, calcite was principally driving the $b_b/(a+b_b)546nm$ through scatter effects and chlorophyll was affecting both $b_b/(a+b_b)436nm$ and $b_b/(a+b_b)546nm$ through absorption and scatter effects. Gordon (personal communication) has modeled the impact of coccoliths and chlorophyll on Lw436 and Lw546 at varying coccolith concentrations and has shown similar behavior to our results. This information will be important for the correction of remotely-sensed images of phytoplankton pigments which are contaminated by high calcite abundance. Conceptually, Lw546 can be used to derive an estimate of coccolith abundance, accurate to about 25,000 coccoliths milliliter^{-1}, while both Lw436 and Lw546 are used to calculate pigment concentration, accurate to +/- 30%. Simultaneous retrieval of

surface pigments and suspended calcite will allow a new level of understanding of the cycling of organic and inorganic carbon in the sea.

References

Aas, E. 1981. The refractive index of phytoplankton. Institute Report Series, Universitetet i Oslo. 46: 61pp.

Aas, 1984. Influence of shape and structure on light scattering by marine particles. Institute Report Series, Universitetet i Olso. 53: 112pp.

Ackleson, S., W. M. Balch, P. M. Holligan. 1994. The response of water-leaving radiance to particulate calcite and pigment concentration: a model for Gulf of Maine coccolithophore blooms. J. Geophys. Res. 99: 7483-7499.

Balch, W. M., K. A. Kilpatrick, and C. R. Trees. The 1991 Coccolithophore Bloom in the Central North Atlantic I. Optical Properties and Factors Affecting Their Distribution. Limnol. Oceanogr. submitted.

Balch, W. M. , P. M. Holligan, S. G. Ackleson, and K. J. Voss. 1991. Biological and optical properties of mesoscale coccolithophore blooms in the Gulf of Maine. Limnol. Oceanogr. 36: 629-643.

Balch, W.M., K.A. Kilpatrick, and P.M. Holligan. 1993. Coccolith formation and detachment by *Emiliania huxleyi* (Prymnesiophyceae). J. Phycol. 29: 566-575.

Berger, W. H. 1976. Biogenous deep sea sediments: production, preservation and interpretation. p. 266-326. In J. P. Riley and R. Chester [eds.], Chemical Oceanography, Vol. 5. Academic Press.

Borstad, G. A., J. F. R. Gower and E. J. Carpenter. 1992. Development of algorithms for remote sensing of marine *Trichodesmium* blooms In E. J. Carpenter [ed.] Marine Pelagic Cyanobacteria: *Trichodesmium* and other diazotrophs. Kluwer.

Bratbak, G., J. K. Egge, and M. Heldal. 1993. Viral mortality of the marine alga Emiliania huxleyi (Haptophyceae) and termination of algal blooms. Mar. Ecol. Prog. Ser., 93: 39-48.

Bricaud, A, J. R. V. Zaneveld, and J. C. Kitchen. 1992. Backscattering efficiency of coccolithophorids: use of a three-layered sphere model. SPIE- The International Society for Optical Engineering, Ocean Optics XI. 1750: 27-33.

Brown, C. and J. Yoder. 1993. Distribution pattern of coccolithophorid blooms in the Western North Atlantic. Cont. Shelf Res. 14:175-198.

Eppley, R. W., R. W. Holmes, and J. D. H. Strickland. 1967. Sinking rates of marine phytoplankton measured with a fluorometer. J. Exp. Mar. Biol. Ecol. 1: 191-208.

Fernandez, E., P. Boyd, P. M. Holligan and D. S. Harbour. 1993. Production of organic and inorganic carbon within a large scale coccolithophore bloom in the north Atlantic Ocean. Mar. Ecol. Prog. Ser. 97: 271-285.

Gordon, H. R. 1987. A bio-optical model describing the distribution of irradiance at the sea surface resulting from a point source embedded in the ocean. Applied Optics 26: 4133-4148.

Gordon, H. R. 1992. Diffuse reflectance of the ocean: influence of nonuniform phytoplankton pigment profile. Applied Optics. 31: 2116-2129.

Gordon, H. and A. Y. Morel. 1983. Remote Assessment of Ocean Color for Interpretation of Satellite Visible Imagery- A Review. Springer-Verlag.

Gordon, H. R., R. C. Smith, and J. R. V. Zaneveld. 1980. Introduction to Ocean Optics. in S. Duntley [ed.], Proceedings of the Society of Photo-Optical Instrumentation Engineers.- Ocean Optics IV. 208: 14-55.

Gordon, H. R., O. B. Brown, R. H. Evans, J. W. Brown, R. C. Smith, K. S. Baker, and D. K. Clark. 1988. A semianalytic radiance model of ocean color. Journal of Geophysical Research 93: 10909-10924.

Holligan, P. M. , M. Viollier, D. S. Harbout, P. Camus, and M. Champagne-Philippe. 1983. Satellite and ship studies of coccolithophore production along a continental shelf edge. Nature 304: 339-342.

Holligan, P. M., R. P. Harris, R. C. Newell, D. S. Harbour, R. N. Head, E. A. S. Lindley, M. I. Lucas, P. R. G. Tranter, and C. M. Weekley. 1984. Vertical distribution and partitioning of organic carbon in mixed, frontal and stratified waters of the English Channel. Mar. Ecol. Prog. Ser. 14: 111-127.

Holligan, P. M., E. Fernandez, J. Aiken, W. M. Balch, P. Boyd, P. H. Burkill, M. Finch, S. B. Groom, G. Malin, K. Muller, D. A. Purdie, C. Robinson, C. Trees, S. Turner, and P. van der Wal. 1993. A biogeochemical study of the coccolithophore, *Emiliania huxleyi*, in the north Atlantic. Global Bio. Cycles 7: 879-900.

Jerlov, N. G. 1976. Marine Optics. Elsevier Scientific Publishing Company.

Kirk, J. T. O. 1981a. Monte carlo study of the nature of the underwater light field in, and the relationships between optical properties of, turbid yellow waters. Aust. J. Mar. Freshwater Res., 32: 517-532.

Kirk, J. T. O. 1981b. Estimation of the scattering coefficient of natural waters using underwater irradiance measurements. Aust. J. Mar. Freshwater Res., 32: 533-539.

Kirk, J. T. O. 1991. Volume scattering function, average cosines, and the underwater light field. Limnol. Oceanogr. 36: 455-467.

Lewis, M. R., O. Ulloa and T. Platt. 1988. Photosynthetic action, absorption, and quantum yield spectra for a natural population of *Oscillatoria* in the North Atlantic. Limnol. Oceanogr. 33: 92-98.

Linschooten, C., J. D. L. van Bleijswijk, P. R. van Emburg, J. P. M. de Vrind, E. S. Kempers, P. Westbroek, and E. W. de Vrind-de Jong. 1991. Role of the light-dark cycle and medium composition on the production of coccoliths by Emiliania huxleyi (Haptophyceae). J. Phycol. 27: 82-86.

MacIsaac, J. J. and R. C. Dugdale. 1972. Interactions of light and inorganic nitrogen in controlling nitrogen uptake in the sea. Deep-Sea Res. 19: 209-232

Margalef, R. 1979. Life-forms of phytoplankton as survival alternatives in an unstable environment. Oceanologica Acta, 1: 493-509.

Morel, A. 1987. Chlorophyll-specific scattering coefficient of phytoplankton, a simplified theoretical approach. Deep Sea Res. 34: 1093-1105.

Morel, A. and A. Bricaud 1980. Theoretical results concerning the optics of phytoplankton, with special reference to remote sensing applications. in Oceanography From Space. J. F. R. Gower ed. Plenum Press: New York. 313-321.

Paasche, E. 1962. Coccolith formation. Nature 193: 1094-1095.

Paasche, E. 1963. The adaptation of the Carbon-14 method for the measurement of coccolith production in *Coccolithus huxleyi,* Physiologia Plantarum, 16: 186-200.

Petzold, T. J. 1972. Volume scattering functions for selected ocean waters. Scripps Inst. Oceanogr. Ref. 72-78.

Pingree, R. D., P. R. Pugh, P. M. Holligan and G. R. Forster. 1975. Summer phytoplankton blooms and red tides along tidal fronts in the approaches to the English Channel. Nature. 258: 672-677.

Reid, F. M. H. 1980. Coccolithophorids of the North Pacific Central Gyre with notes on their vertical and seasonal distribution. Micropaleontology. 26: 151-176.

Robinson, J. E., C. Robinson, D. R. Turner, P. M. Holligan, A. J. Watson, P. Boyd, E. Fernandez, and M. Finch. 1994. The impact of a coccolithophore bloom on oceanic carbon uptake in the N. E. Atlantic during summer 1991. Deep Sea Research. 41: 297-314.

Seibold, E. and W. H. Berger. 1982. The Sea Floor. Springer-Verlag.

van de Hulst, H. C. 1981. Light scattering by small particles. Dover Publications, Inc.

Winter, A. and W. G. Siesser. 1994. Coccolithophores. Cambridge University Press.

Yoder, J. A., S. G. Ackleson, R. T. Barber, P. Flament, and W. M. Balch. 1994. A line in the sea. Nature. 371: 689-692.

Table 1- List of symbols, with definitions and units . Values are given when applicable.

a	absorption coefficient (m^{-1})
ap	particulate absorption coefficient (m^{-1})
a*	Chlorophyll *a*-specific absorption (m^{-2} (mg chl^{-1}))
b	Scattering coefficient (m^{-1})
b_{chl}	scattering due to chlorophyll *a* (m^{-1})
$b^*\lambda$	calcite-specific scattering coefficient (m^2 (mg calcite C)$^{-1}$)
b_b	backscattering coefficient (m^{-1})
b_b'	calcite-specific backscattering coefficient (m^{-1})
b_{bchl}	chlorophyll *a*-specific backscattering coefficient (m^{-1})
B_c	scattering coefficient when chlorophyll *a* +phaeopigment =1 mg m^{-3}
$\tilde{b}_b$	b_b/b (dimensionless)
$\tilde{b}_{b\,chl}$	b_{bchl}/b_{chl} (dimensionless)
C_{CaCO3}	concentration of calcite as carbon (μg liter^{-1})
c	beam attenuation coefficient (m^{-1})
$c_{calcite}$	density of calcite (2.711×10^6 g m^{-3})
C	concentration of chlorophyll plus phaeopigment (mg m^{-3})
Chl	concentration of chlorophyll (mg m^{-3})
d	particle diameter (m)
γ	ratio of calcite:chlorophyll by mass (mg calcite C/ mg chlorophyll *a*)
$G(\mu_o)$	fraction of scattering to vertical attenuation
Kd	vertical attenuation coefficient for downward irradiance (m^{-1})
Kd(zm)	vertical attenuation coefficient for downward irradiance at mid-point of euphotic zone (m^{-1})
Kd(avg)	average Kd in euphotic zone (m^{-1})
λ	wavelength (nm)
Lw	water-leaving radiance (W m^{-2} sr^{-1})

n	index of refraction (=1.58 for calcite)
n_w	index of refraction of water (=1.33)
n'	imaginary part of the refractive index
N_{cocco}	concentration of coccoliths (per milliliter^{-1})
N_{cells}	concentration of coccolithophore cells (per milliliter^{-1})
μ_o	cosine of the zenith angle of refracted solar photons just beneath the surface
m	relative refractive index (n/n_w)
Qa	absorption efficiency
Qb	scattering efficiency
Qc	attenuation efficiency
ρ	dimensionless parameter relating the size of particles to the wavelength of light and their relative refractive index $[2\pi (d/\lambda) (m-1)]$

Table 2. Statistical summary of linear optical relationships found during the BOFS cruise. Table provides the name of the independent variable (Ind. Var.) and its associated standard error of prediction, Dependent variable (Dep. Var.), number of points, least-squares fit slope, standard error (s.e.) of the slope, least-squares fit intercept (Int), standard error of the intercept, coefficient of determination, F statistic (equal to the regression mean square/residual mean square), and P, the probability that the slope is equal to 0 (* indicates $P<0.001$, Type 1 error). When regressions were performed using log transformed variables, this is shown in the first two columns. The units of the variables are N_{cell} (cells milliliter^{-1}), N_{cocco} (coccoliths milliliter^{-1}), C_{CaCO3}(mg C liter^{-1}), b_b'(m^{-1}), b (m^{-1}), b/a (dimensionless), and γ (mg calcite C/mg chlorophyll a).

Ind Var	s.e. Y	Dep Var	n	Slope	s.e.	Int	s.e	r^2	F	P
Log[N_{cell}]	0.31	Log[N_{cocco}]	172	0.91	3.72E-2	1.60	1.21E-1	0.779	600	*
[C_{CaCO3}]	51.69	[N_{cocco}]	102	1.05E-3	6.93E-5	48.27	7.41	0.690	231	*
b_b'436	9.61E-3	[N_{cocco}]	61	1.84E-7	1.82E-8	3.36E-3	1.82E-3	0.634	102	*
b_b'546	8.35E-3	[Ncocco]	61	1.35E-7	1.58E-8	3.06E-3	1.58E-3	0.556	74	*
b_b'436	5.24E-3	[C_{CaCO3}]	118	1.76E-4	6.33E-6	-4.67E-3	7.17E-4	0.866	775	*
b_b'546	4.33E-3	[CCaCO3]	118	1.36E-4	5.23E-6	-3.61E-3	5.92E-4	0.849	674	*
b436	0.552	[C_{CaCO3}]	140	9.37E-3	5.28E-4	4.42E-1	7.23E-2	0.695	315	*
b546	0.492	[C_{CaCO3}]	143	8.41E-3	4.64E-4	4.10E-1	6.28E-2	0.700	328	*
b546/a546	7.70	γ	135	6.69E-2	6.63E-3	7.62	1.03	0.433	102	*
b546/a546†	5.28	γ	83	5.94E-2	5.20E-3	13.09	0.943	0.617	130	*

† for data where b546/a546 >10 only.

Table 3-Results of dilution experiments at various locations within the mesoscale coccolithophore bloom.

Date 1991	Lat	Lon	Depth (m)	n	Slope x10^{-10}	Int x10^{-3}	r^2	Slope x10^{-10}	Int x10^{-3}	r^2
					436nm			546nm		
6/22	61.5	22.6	12	7	5.34	1.76	0.99	3.72	1.3	0.99
6/24	60.9	22.9	2	6	2.58	0.31	0.98	1.82	-3.01	0.97
6/25	60.9	23.9	2	7	4.66	0.97	0.91	3.56	0.59	0.91
6/27	61.2	15.2	2	5	1.35	0.50	0.99	1.01	1.5	0.84
6/29	61.1	15.0	2	7	1.58	-0.98	0.95	1.22	-0.80	0.97
6/29b	61.0	15.6	2	5	2.65	0.33	0.99	2.07	0.036	1.00
6/30	62.0	15.2	2	6	1.96	1.19	0.99	1.54	0.43	0.99

Table 4- Detached coccoliths per plated coccolithophore and coccolith-specific backscattering (m^{-1} per coccolith) as a function of bloom age (d). Column 2 assumes that the bloom began on June 10, 1991, the date of the last clear satellite image (Balch et al., submitted). Data are only given for stations where b_b' was measured. This table demonstrates how normalization of b_b' by the number of detached coccoliths, not including those attached to cells, can cause an increase in the coccolith-specific backscattering at early stages of bloom development.

Date June '91	Bloom Age Days	Detached coccoliths per plated coccolithophore	b_b* $x10^{-13}$ m^2/det. coccolith
22	12	7.65	3.72
24	14	11.94	1.82
25	15	9.07	3.56
27	17	19.49	1.01
29	19	18.48	2.07
29	19	28.29	1.22
30	20	36.99	1.54

Figure Legends

Fig. 1A) Relationship between detached coccolith concentration and numbers of *E. huxleyi* coccoliths per liter. Line drawn is a least squares fit. B) Suspended calcite concentration versus coccolith concentration. Line represents a least-squares fit to the data. See text for equation.

Fig. 2- Calcite-specific backscattering at A) 436nm and B) 546nm, as a function of concentration of suspended calcite. Lines represent least-squares fits to the data (see Table 2 for equations).

Fig. 3- Results of seven dilution experiments in which seawater (containing coccolithophores and detached coccoliths) was serially diluted, and calcite-dependent backscattering was estimated at A) 436nm and B) 546nm wavelengths. The least squares fit is shown for each experiment along with the date. See Table 3 for the slope and intercept values for each experiment. Note, the ordinate scales are different. The symbols represent the following sample dates (during 1991) : +=6/22, Δ=6/24, O=6/25, ●=6/27, ▼ = 6/29, ❑ =6/29b, X=6/30.

Fig. 4- Scatter at 436 nm and 546 nm versus the concentration of calcite carbon. Lines represent least-squares fits; the fitted slopes and intercepts are given in Table 2.

Fig. 5- Calcite-specific scatter at 546nm versus coccolith concentration showing trend towards low b* values at high detached coccolith concentrations. The solid line represents the slope in Fig. 4b. The dashed line represents the theoretical maximum b* calculated using anomalous diffraction theory (van de Hulst 1981). See discussion for details of the calculation.

Fig. 6- Modeled ratio for b_b'/b_btot at 436 nm as a function of A) coccolith concentration and B) calcite concentration. Modeled ratio for b_b'/b_btot at 546nm as a function of C) coccolith concentration and D)calcite concentration. Each line assumes a chlorophyll *a* concentration, from top to bottom, of 0.01, 0.03, 0.1,0.3, 1.0, 3.0, 10.0 μg/liter. Data points from the mesoscale coccolithophore bloom are shown as Δ's.

Fig. 7- Theoretical calcite-specific scatter coefficient for calcite spheres versus sphere diameter, calculated using the anomalous diffraction theory (van de Hulst 1981). See text for details of this calculation. The size ranges of various calcium carbonate particles found in the sea are shown for reference (see Berger 1976, Seibold and Berger 1982, Winter and Siesser 1994).

Fig. 8- Values of $b_b/(a+b_b)$ at 546 nm plotted versus $b_b/(a+b_b)$ at 436 nm. Concentrations of coccoliths contoured which show high dependence of $b_b/(a+b_b)$ 546 on coccolith abundance and relative independence of $b_b/(a+b_b)$ at 436 nm to coccolith abundance. The values $b_b/(a+b_b)$ are expected to act similarly to reflectance and water-leaving irradiance at the respective wavelengths.

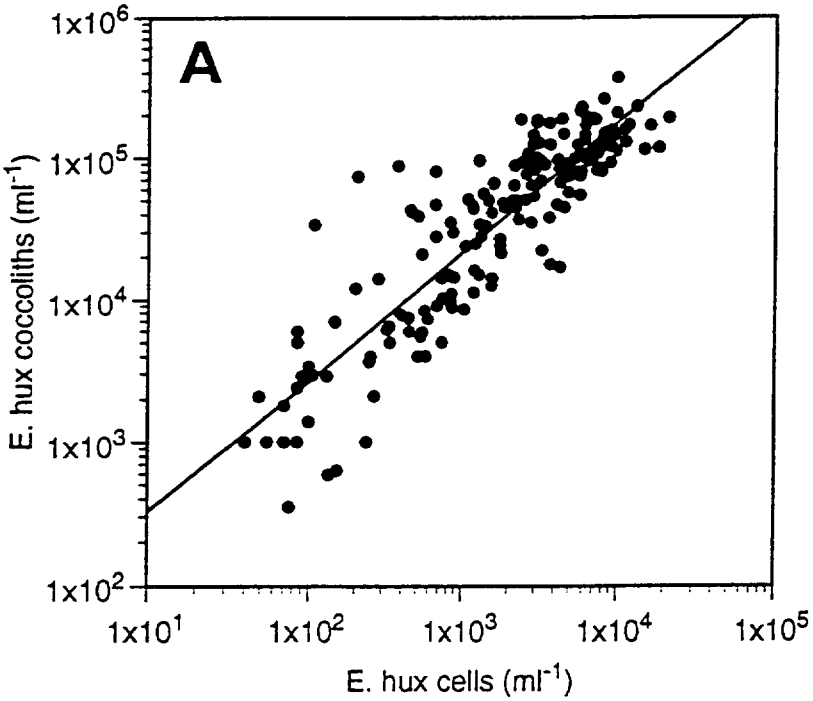
A
E. hux coccoliths (ml-1)
1x10^6
1x10^5
1x10^4
1x10^3
1x10^2
1x10^1
1x10^2
1x10^3
1x10^4
1x10^5
E. hux cells (ml-1)

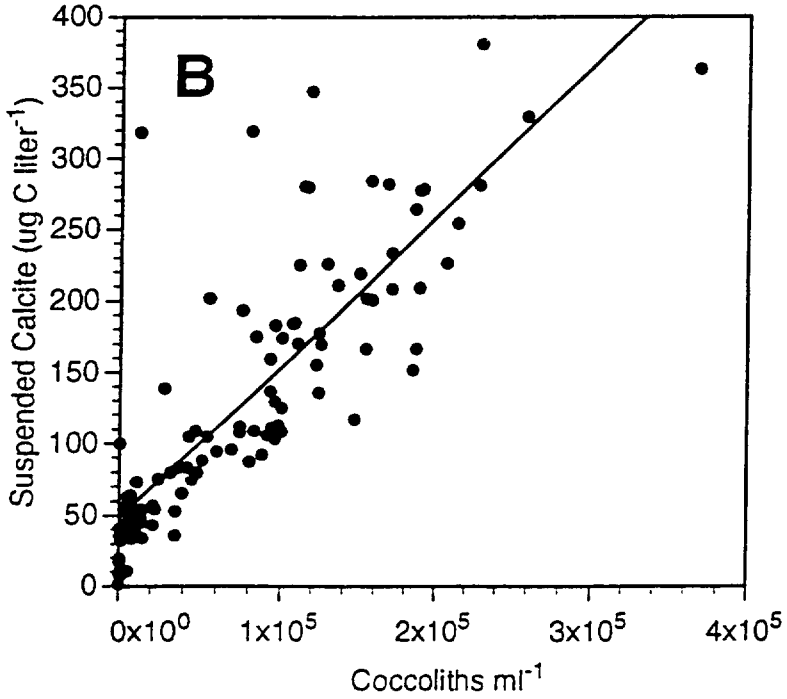
B
Suspended Calcite (ug C liter-1)
400
350
300
250
200
150
100
50
0
0x10^0
1x10^5
2x10^5
3x10^5
4x10^5
Coccoliths ml-1

Fig 1

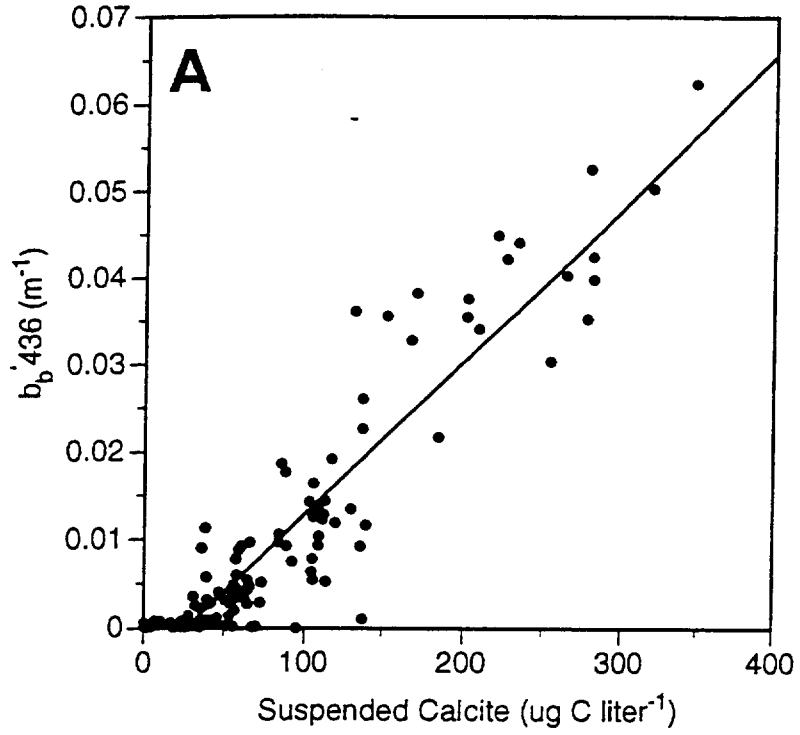
A
0.07
0.06
0.05
0.04
0.03
0.02
0.01
0
b_b'436 (m^{-1})
0
100
200
300
400
Suspended Calcite (ug C $liter^{-1}$)

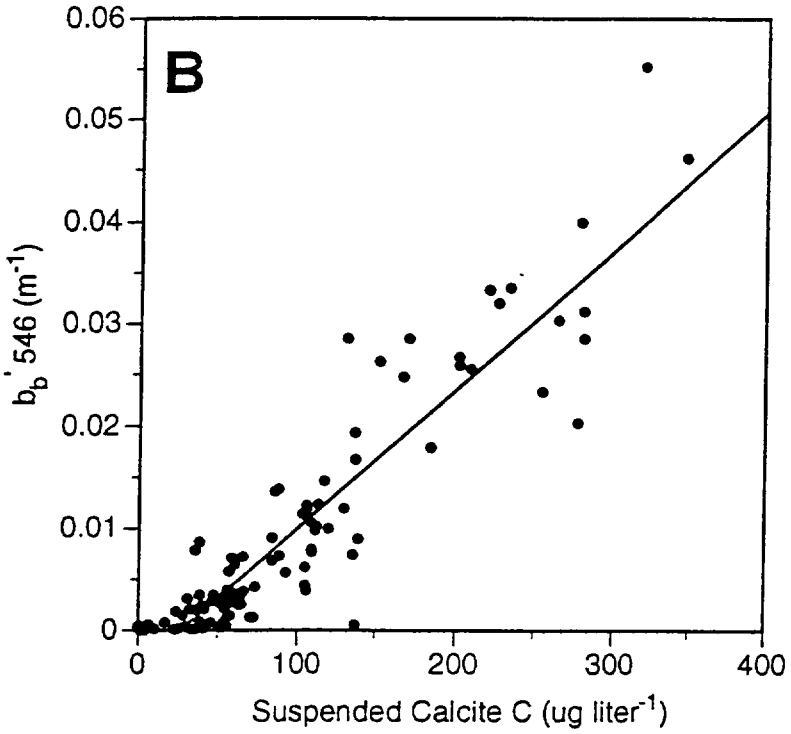
B
0.06
0.05
0.04
0.03
0.02
0.01
0
b_b'546 (m^{-1})
0
100
200
300
400
Suspended Calcite C (ug $liter^{-1}$)

Fig 2

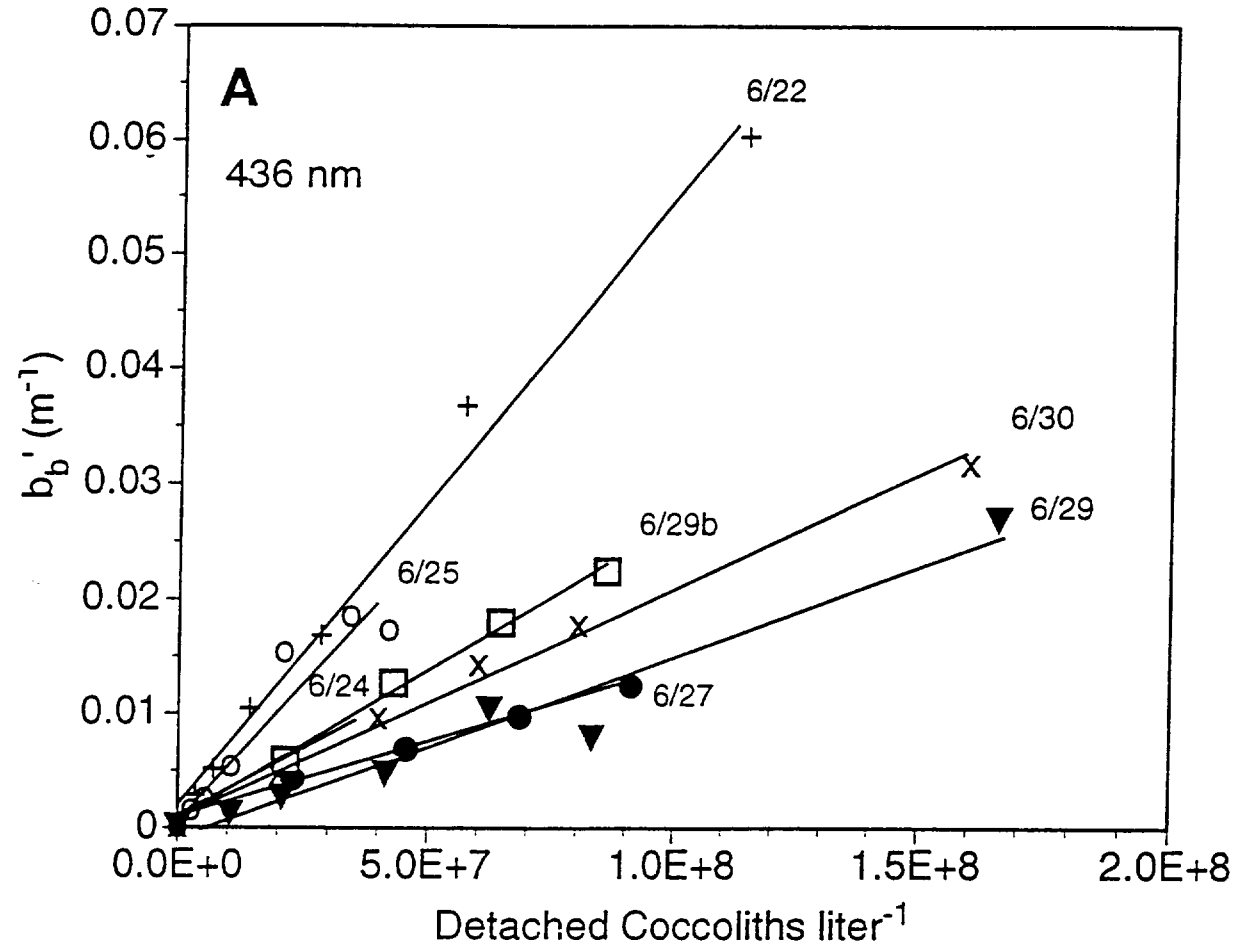
A
436 nm
6/22
6/30
6/29
6/29b
6/25
6/24
6/27
0.07
0.06
0.05
0.04
0.03
0.02
0.01
0
b_b' (m^{-1})
0.0E+0
5.0E+7
1.0E+8
1.5E+8
2.0E+8
Detached Coccoliths $liter^{-1}$

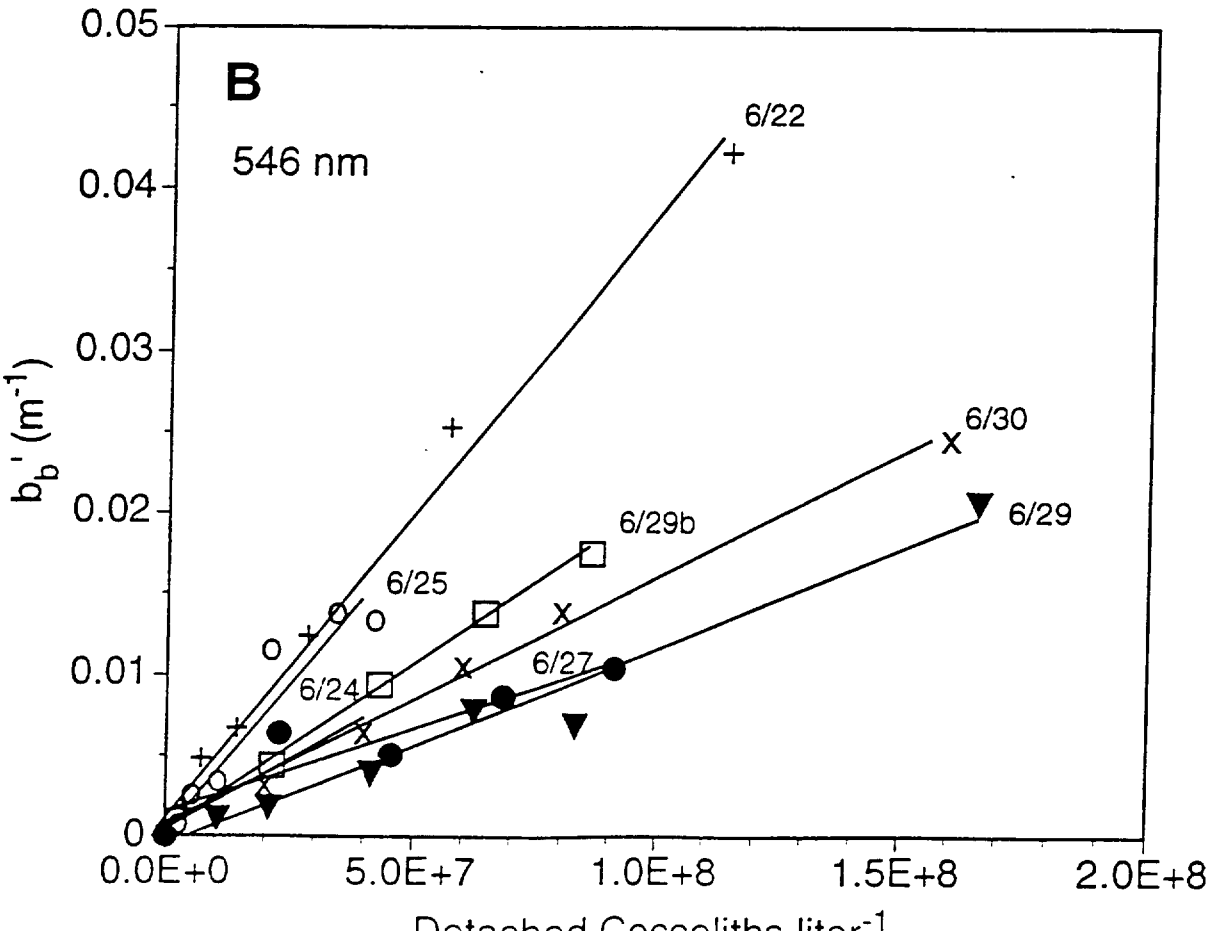
B
546 nm
6/22
6/30
6/29
6/29b
6/25
6/24
6/27
0.05
0.04
0.03
0.02
0.01
0
b_b' (m^{-1})
0.0E+0
5.0E+7
1.0E+8
1.5E+8
2.0E+8

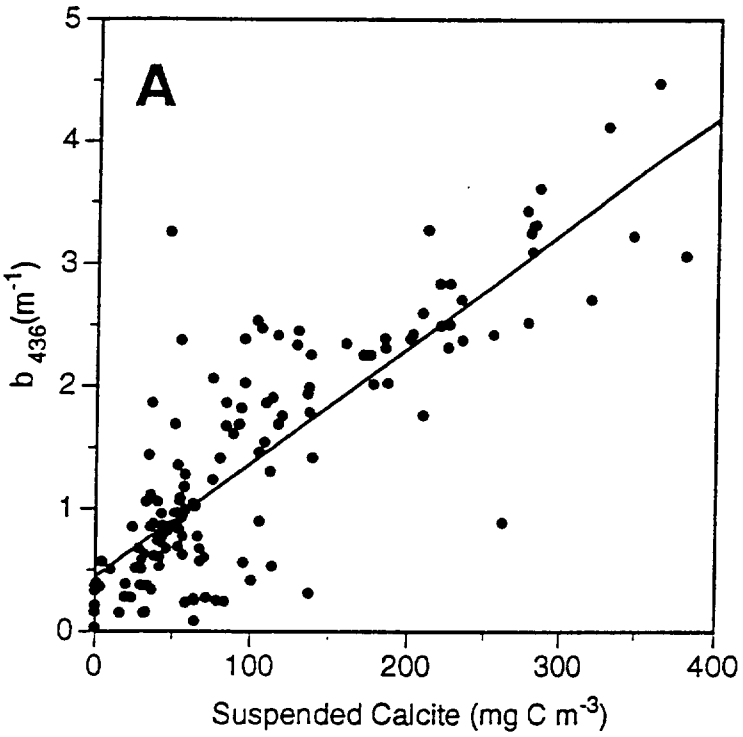
A
5
4
3
2
1
0
$b_{436}(m^{-1})$
0
100
200
300
400
Suspended Calcite (mg C m^{-3})

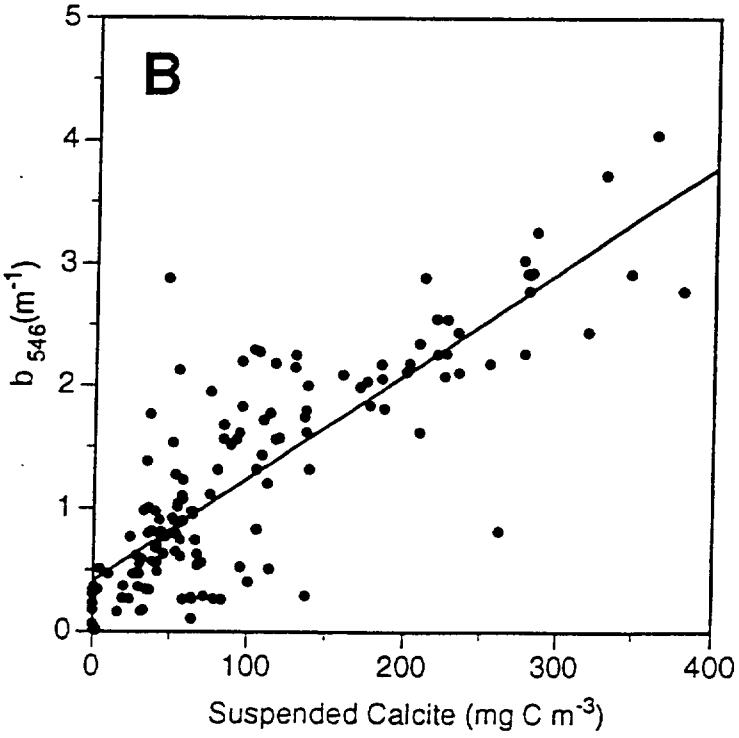
B
5
4
3
2
1
0
$b_{546}(m^{-1})$
0
100
200
300
400
Suspended Calcite (mg C m^{-3})

Fig 4

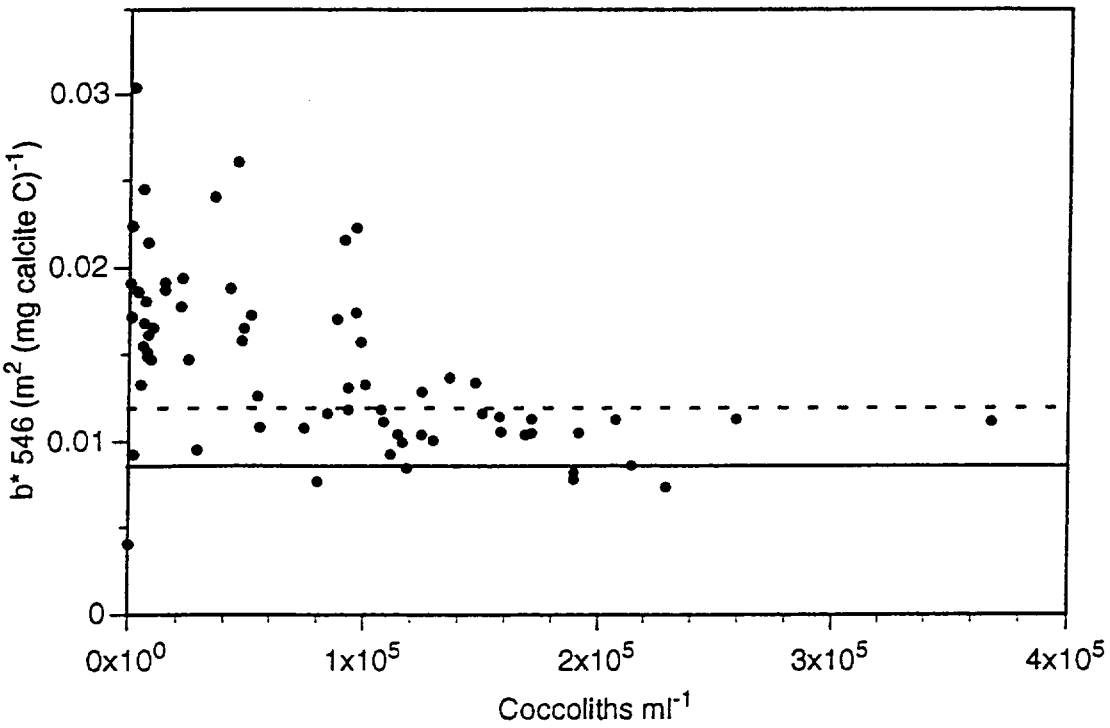
0.03
0.02
0.01
0
b* 546 (m^2 (mg calcite C)$^{-1}$)
0x10^0
1x10^5
2x10^5
3x10^5
4x10^5
Coccoliths ml^{-1}

Fig 5

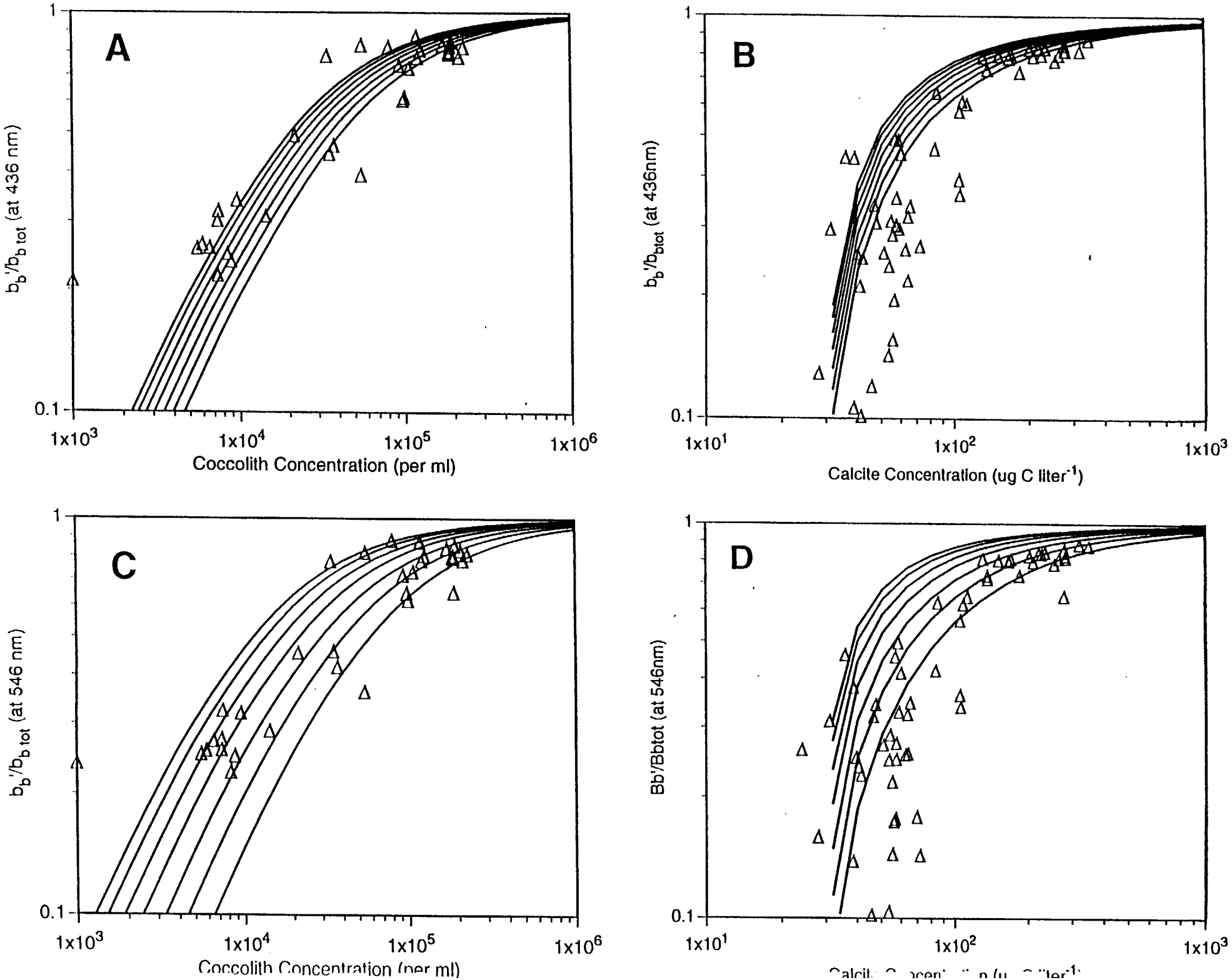
A
B
C
D
1
0.1
$b_b'/b_{b\,tot}$ (at 436 nm)
b_b'/b_{btot} (at 436nm)
$b_b'/b_{b\,tot}$ (at 546 nm)
Bb'/Bbtot (at 546nm)
1x10^3
1x10^4
1x10^5
1x10^6
1x10^1
1x10^2
1x10^3
Coccolith Concentration (per ml)
Calcite Concentration (ug C liter^-1)

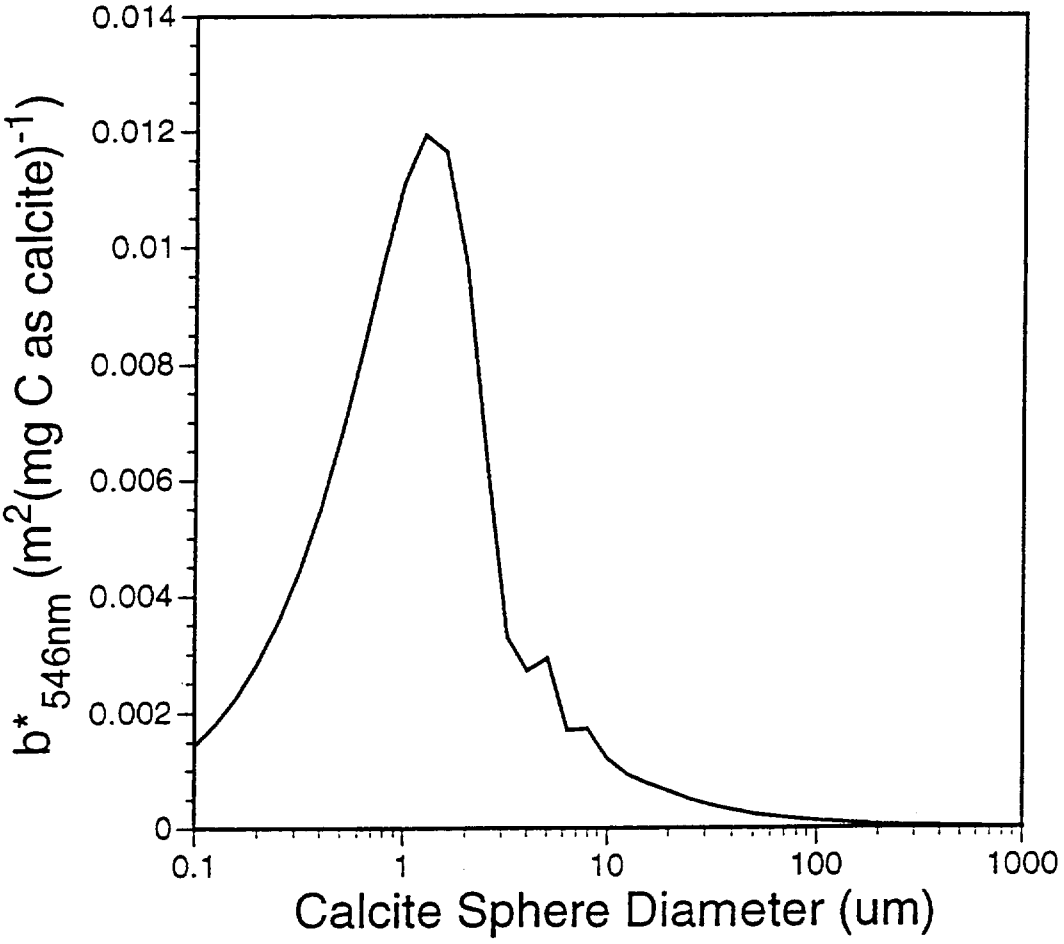

Range in diameter of E. huxleyi coccoliths

Range in diameter of foraminifera tests

Range in diameter of most coccoliths

Pteropod shells and oolites ~1-3mm in diameter

Size range of coccospheres

Range in Length of Aragonite Needles

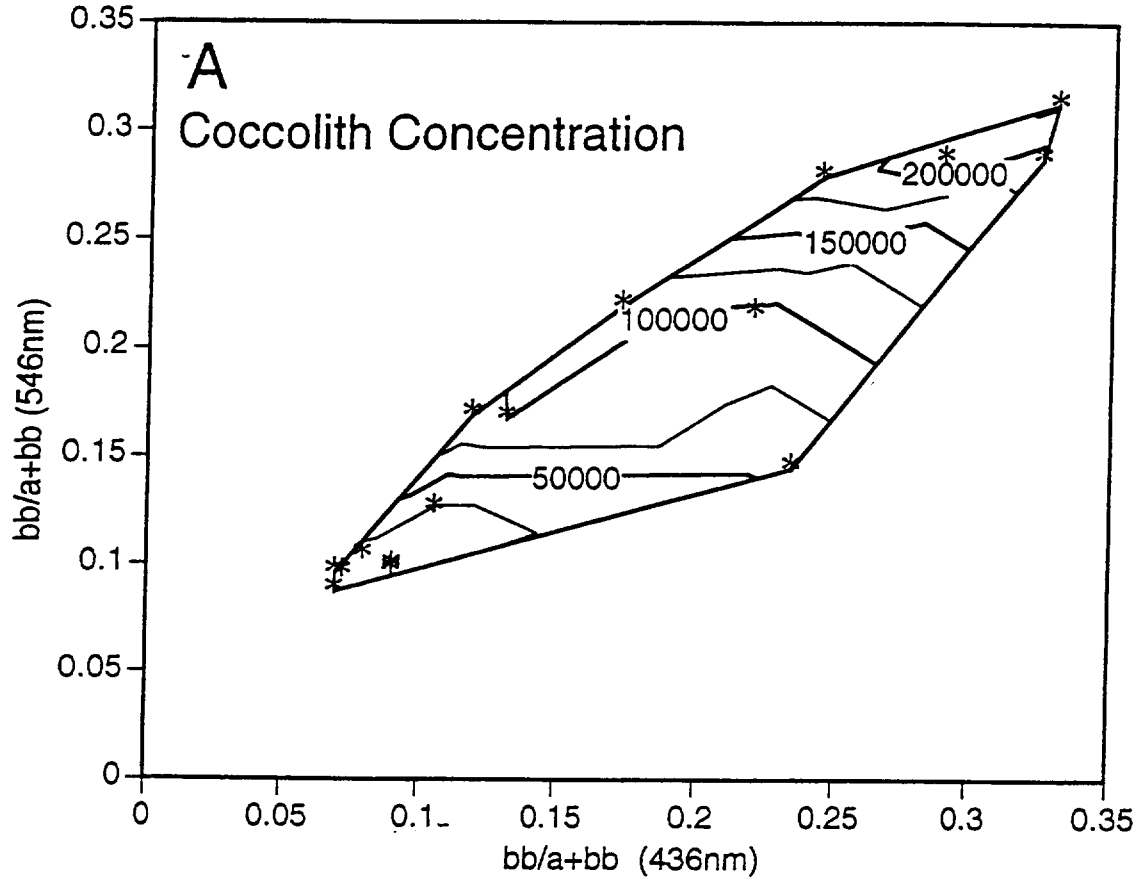
A
Coccolith Concentration
200000
150000
100000
50000
bb/a+bb (546nm)
bb/a+bb (436nm)
0.35
0.3
0.25
0.2
0.15
0.1
0.05
0
0
0.05
0.1
0.15
0.2
0.25
0.3
0.35

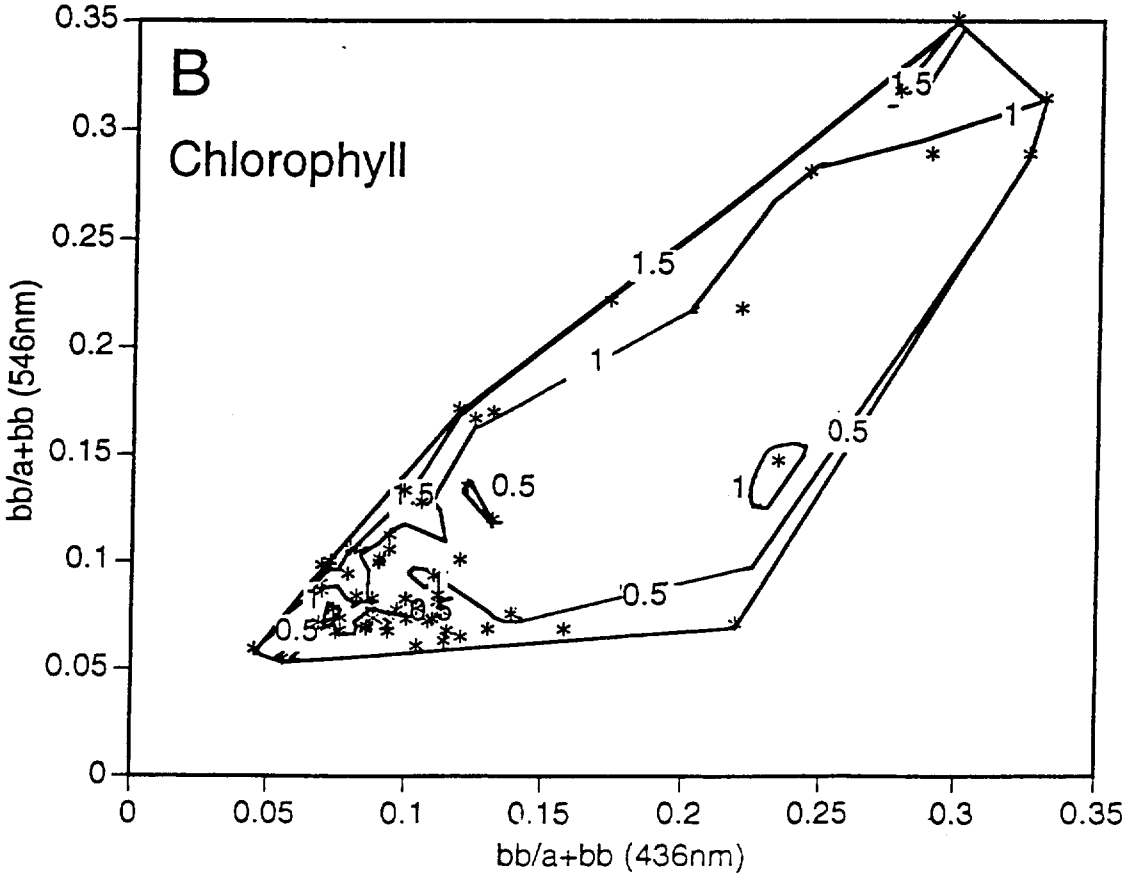
B
Chlorophyll
1.5
1
0.5
bb/a+bb (546nm)
bb/a+bb (436nm)
0.35
0.3
0.25
0.2
0.15
0.1
0.05
0
0
0.05
0.1
0.15
0.2
0.25
0.3
0.35